

## Parahilgardite, $\text{Ca}_6[\text{B}_5\text{O}_9]_3\text{Cl}_3 \cdot 3\text{H}_2\text{O}$ : a triclinic piezoelectric zeolite-type pentaborate

CHE'NG WAN AND SUBRATA GHOSE

Department of Geological Sciences  
University of Washington  
Seattle, Washington 98195

### Abstract

Parahilgardite,  $\text{Ca}_6[\text{B}_5\text{O}_9]_3\text{Cl}_3 \cdot 3\text{H}_2\text{O}$  from Iberville Parish, Louisiana is triclinic, mildly piezoelectric, space group *P1*, with unit cell dimensions:  $a = 17.495(4)$ ,  $b = 6.487(1)$ ,  $c = 6.313(1)\text{\AA}$ ;  $\alpha = 60.77(1)$ ,  $\beta = 79.56(1)$ ,  $\gamma = 83.96(1)^\circ$ ;  $Z = 1$ . The *R*-factor is 0.020 for 4490 reflections. The absolute configuration and hydrogen positions have been determined. The structure of parahilgardite is a three dimensional framework, whose building blocks are three crystallographically distinct pentaborate polyanions  $[\text{B}_5\text{O}_{12}]^{9-}$ , each consisting of three  $(\text{BO}_4)$  tetrahedra and two  $(\text{BO}_3)$  triangles. These polyanions, two of which are in *l* and one in *d* configuration, form three distinct single chains by sharing tetrahedral corners along the *c* axis. By sharing tetrahedral and triangular corners, each chain is connected to four adjacent chains, resulting in an open framework with channels parallel to all three axes, where calcium and chlorine atoms and the water molecules are located. The calcium polyhedra are hexagonal bipyramids, which are connected to form an open sheet. The water molecules are hydrogen bonded with chlorine atoms in quasi-linear chains parallel to the *c* axis.

### Introduction

Hydrated borate polyanions can polymerize by splitting out water molecules to form chains, sheets and three dimensional frameworks (Christ, 1960; Christ and Clark, 1977). Among the pentaborates, the isolated pentaborate polyanions  $[\text{B}_5\text{O}_6(\text{OH})_6]^{3-}$ , formed by corner sharing of three borate tetrahedra and two borate triangles exist in ulexite,  $\text{NaCaB}_5\text{O}_6(\text{OH})_6 \cdot 5\text{H}_2\text{O}$  (Clark and Appleman, 1964; Ghose *et al.*, 1978); they can polymerize to form a chain by sharing an oxygen atom common to a borate triangle of one polyanion and a tetrahedron of the next, which occurs in probertite,  $\text{NaCaB}_5\text{O}_7(\text{OH})_4 \cdot 3\text{H}_2\text{O}$  (Rumanova *et al.*, 1966). These polyanions, further linked into sheets, occur in heidornite,  $\text{Na}_2\text{Ca}_3\text{Cl}[\text{B}_5\text{O}_8(\text{OH})_2][\text{SO}_4]_2$  (Burzlaff, 1967) and synthetic  $\text{Na}_3\text{B}_5\text{O}_8(\text{OH})_2 \cdot \text{H}_2\text{O}$  (Menchetti and Sabelli, 1977). The culmination of this polymerization process results in an anhydrous pentaborate framework, which occurs in  $\text{Ca}_2\text{B}_5\text{O}_9\text{Br}$  (Lloyd *et al.*, 1973), in hilgardite,  $\text{Ca}_2\text{B}_5\text{O}_9\text{Cl} \cdot \text{H}_2\text{O}$  and parahilgardite,  $\text{Ca}_6[\text{B}_5\text{O}_9]_3\text{Cl}_3 \cdot 3\text{H}_2\text{O}$  (Ghose and Wan, 1977, 1979) and in the triclinic hilgardite-type phase  $\text{Ca}_2[\text{B}_5\text{O}_9]\text{Cl} \cdot \text{H}_2\text{O}$  (Rumanova *et al.*, 1977). We have recently described the crystal structure of hilgardite (Ghose and Wan, 1979). In this paper, we present the details of the parahilgardite structure.

### Occurrence and chemical composition

Hilgardite and parahilgardite were found in the insoluble residues from a brine well in the Choctaw Salt Dome, Iberville Parish, Louisiana (Hurlbut and Taylor, 1937, Hurlbut, 1938). Parahilgardite is triclinic. It is found only as oriented intergrowths on hilgardite, which is monoclinic (crystal class *m*). The intergrowths consist of two partly merged individual crystals of parahilgardite, one right-handed and one left-handed and apparently in twin-position.

From a chemical analysis, Hurlbut (1938) assigned the composition,  $\text{Ca}_8(\text{B}_6\text{O}_{11})_3\text{Cl}_4 \cdot 4\text{H}_2\text{O}$  to parahilgardite. Braitsch (1959) described a new strontiohilgardite phase, whose unit cell volume is one-third that of parahilgardite; on this basis, he suggested that the chemical composition of parahilgardite is  $3[\text{Ca}_2\text{B}_5\text{O}_8(\text{OH})_2\text{Cl}]$ . Based on the crystal structure determination, Ghose and Wan (1977) showed that the correct chemical composition of parahilgardite is  $3[\text{Ca}_2\text{B}_5\text{O}_9\text{Cl} \cdot \text{H}_2\text{O}]$ .

### Crystal data

Hurlbut (1938) determined the crystal class of parahilgardite to be triclinic non-centrosymmetric (piezoelectric), space group *P1*. However, his unit cell dimensions ( $a = 11.24$ ,  $b = 22.28$  and  $c = 6.20$  kX,  $\alpha = 90^\circ 00'$ ,  $\beta =$

90°00' and  $\gamma = 91^{\circ}12'$ ) were apparently incorrect. The correct dimensions were determined by Braitsch (1959) and are in good agreement with those determined by us, based on a least-squares refinement of  $2\theta$  values ranging between 25 and 50° for 15 reflections from a spherical crystal (diameter 0.28 mm) measured on the computer controlled single crystal X-ray diffractometer (Syntex P $\bar{I}$ ) with MoK $\alpha$  radiation. The unit cell dimensions are:  $a = 17.495(4)$ ,  $b = 6.487(1)$ ,  $c = 6.313(1)\text{\AA}$ ,  $\alpha = 60.77(1)$ ,  $\beta = 79.56(1)$ ,  $\gamma = 83.96(1)^{\circ}$ , unit cell volume =  $614.8(2)\text{\AA}^3$ , space group  $P1$ ,  $Z = 1$ . The measured and calculated densities are 2.71 (Hurlbut, 1938) and  $2.69\text{ gm cm}^{-3}$  respectively and  $\mu_{\text{MoK}\alpha} = 16.90\text{ cm}^{-1}$ .

### Determination and refinement of the structure

The intensity data were collected from the same crystal sphere on the Syntex P $\bar{I}$  diffractometer, using MoK $\alpha$  radiation monochromatized by reflection from a graphite "single" crystal and scintillation counter. All reflections within  $2\theta \leq 65^{\circ}$  were measured with MoK $\alpha$  radiation using the  $2\theta - \theta$  variable scan method, the minimum scan rate being 2°/min (50 kV, 12 mA). Out of a total of 4490 reflections measured, 135 reflections were less than  $3\sigma(I)$ , where  $\sigma(I)$  is the standard deviation of the measurement of the intensity,  $I$  as determined by the counting statistics. For intensities less than  $0.7\sigma(I)$ ,  $I$  was set equal to  $0.7\sigma(I)$ , whether the measured intensity was positive or negative.

The intensity data were converted to structure factors after correction for Lorentz, polarization and absorption factors. The positions of the six calcium and three chlorine atoms were determined from the three dimensional Patterson map. The structure factors calculated using these atomic positions yielded an  $R$  factor of 0.35. Successive three-dimensional Fourier and difference Fourier syntheses indicated the positions of the boron and oxygen atoms. Subsequent full matrix least-squares refinement using isotropic temperature factors reduced the  $R$  factor to 0.028. A difference Fourier syntheses calculated at this stage yielded the positions of the six hydrogen atoms, which were stereochemically reasonable.

Further least-squares refinement was carried out by the CRYLSQ program incorporated in the X-RAY SYSTEM (Stewart *et al.*, 1972) using anisotropic temperature factors for all atoms, except hydrogens, for which isotropic temperature factors were used. The atomic scattering factors for Ca, B, O and Cl were taken from Cromer and Mann (1968) and for H from Stewart *et al.* (1965). Anomalous dispersion corrections were applied according to Cromer and Liberman (1970). The observed structure factors ( $F_o$ ) were weighted by the formula  $1/\sigma^2(F_o)$ , where  $\sigma(F_o)$  is the standard deviation of the observed structure factor,  $F_o$ , as determined by the counting statistics. Due to the large dimensions of the problem (66 atoms, 565 variables, 4490 reflections), the final refinement was carried out in 4 blocks; the calcium and the chlorine atoms and the water molecules were in the first

Table 1. Parahilgardite: atomic positional parameters and equivalent isotropic temperature factors (with standard deviations in parentheses)

ATOM	X	Y	Z	*B <sub>eq</sub> /B(Å) <sup>2</sup>
CA(1)	0	0	0	0.81
CA(2)	0.18463(3)	0.56531(8)	0.96931(9)	0.81
CA(3)	0.33334(3)	0.00002(9)	0.33482(9)	0.86
CA(4)	0.51576(3)	0.43129(9)	0.86912(9)	0.77
CA(5)	0.66644(3)	0.98093(9)	0.67773(9)	0.83
CA(6)	0.84599(3)	0.52972(9)	0.65317(9)	0.86
CL(1)	0.02582(4)	0.52911(11)	0.11807(12)	1.24
CL(2)	0.35067(4)	0.48145(11)	0.98505(13)	1.19
CL(3)	0.68142(4)	0.49631(11)	0.81316(12)	1.13
B(1)	0.0405(1)	0.0022(4)	0.5211(4)	0.61
B(2)	0.1506(1)	0.8968(4)	0.2989(4)	0.48
B(3)	0.1743(1)	0.1188(4)	0.5017(4)	0.53
B(4)	0.2246(1)	0.0452(4)	0.8756(4)	0.50
B(5)	0.1820(1)	0.4510(4)	0.5692(4)	0.63
B(6)	0.3739(1)	0.0113(4)	0.8501(4)	0.59
B(7)	0.4838(1)	0.1049(4)	0.5276(4)	0.51
B(8)	0.5074(1)	0.8812(4)	0.9527(4)	0.54
B(9)	0.5577(1)	0.9458(4)	0.2570(4)	0.42
B(10)	0.5139(1)	0.5458(4)	0.3556(4)	0.59
B(11)	0.7071(1)	0.9615(4)	0.2081(4)	0.57
B(12)	0.8178(1)	0.8571(4)	0.9856(4)	0.53
B(13)	0.8399(1)	0.0793(4)	0.1890(4)	0.53
B(14)	0.8905(1)	0.0108(4)	0.5597(4)	0.48
B(15)	0.8459(1)	0.4128(4)	0.2559(4)	0.65
O(1)	0.939(1)	0.0491(3)	0.6294(3)	0.82
O(2)	0.9667(1)	0.9929(3)	0.6355(3)	0.89
O(3)	0.0643(1)	0.9485(3)	0.3344(3)	0.90
O(4)	0.1643(1)	0.6742(3)	0.5304(3)	0.90
O(5)	0.1698(1)	0.8790(3)	0.0782(3)	0.63
O(6)	0.1938(1)	0.0804(3)	0.2928(3)	0.63
O(7)	0.1810(1)	0.3785(3)	0.4005(3)	0.80
O(8)	0.2304(1)	0.9903(3)	0.6739(3)	0.59
O(9)	0.1971(1)	0.2945(3)	0.8002(3)	0.79
O(10)	0.3002(1)	0.0133(3)	0.9585(3)	0.86
O(11)	0.4280(1)	0.9680(3)	0.0024(3)	0.77
O(12)	0.3972(1)	0.0630(3)	0.6094(3)	0.71
O(13)	0.5266(1)	0.9151(3)	0.7072(3)	0.58
O(14)	0.5027(1)	0.1199(3)	0.2894(3)	0.61
O(15)	0.4983(1)	0.3237(3)	0.5374(3)	0.78
O(16)	0.5641(1)	0.0003(3)	0.0002(3)	0.56
O(17)	0.5116(1)	0.6203(3)	0.1134(3)	0.75
O(18)	0.6331(1)	0.9677(3)	0.3137(3)	0.86
O(19)	0.5301(1)	0.7001(3)	0.4295(3)	0.79
O(20)	0.7608(1)	0.9867(3)	0.3225(3)	0.80
O(21)	0.7307(1)	0.3087(3)	0.0199(3)	0.86
O(22)	0.8324(1)	0.6387(3)	0.2141(3)	0.82
O(23)	0.8376(1)	0.8386(3)	0.7649(3)	0.64
O(24)	0.8595(1)	0.0452(3)	0.9769(3)	0.62
O(25)	0.8428(1)	0.3400(3)	0.0883(3)	0.78
O(26)	0.8975(1)	0.9576(3)	0.3562(3)	0.56
O(27)	0.8595(1)	0.2559(3)	0.4884(3)	0.77
O(W1)	-0.0138(1)	0.4338(4)	0.6971(4)	1.81
O(W2)	0.3392(1)	0.5966(3)	0.4420(4)	1.61
O(W3)	0.6725(1)	0.3833(3)	0.3809(4)	1.73
H(1)	0.008(3)	0.460(9)	0.527(10)	5.49
H(2)	0.001(3)	0.501(8)	0.798(9)	4.14
H(3)	0.330(3)	0.575(8)	0.302(9)	6.15
H(4)	0.355(3)	0.485(9)	0.597(9)	5.01
H(5)	0.679(3)	0.409(8)	0.214(9)	4.24
H(6)	0.680(3)	0.489(9)	0.455(9)	5.08

\*  $B_{eq} = (B_{11} + B_{22} + B_{33})/3$  calculated from  $u_{ij}$ 's.

block, all the boron atoms in the second, and half of the oxygen atoms each in the third and the fourth block. The final  $R$  factor for all 4490 reflections is 0.020. The final atomic positional and anisotropic thermal parameters are listed in Tables 1 and 2<sup>1</sup> respectively. The observed and

<sup>1</sup> To receive a copy of Table 2 and Table 3 order document AM-83-224 from the Business Office, Mineralogical Society of America, 2000 Florida Ave., N.W., Washington, D.C. 20009. Please remit \$1.00 in advance for microfiche.

calculated structure factors are listed in Table 3<sup>1</sup>. The interatomic distances and their standard deviations, which include the standard deviations in unit cell dimensions, are listed in Table 4. The average standard deviation in Ca–O, Ca–Cl, B–O and O–H distances are 0.002, 0.001, 0.002, and 0.04 Å and in O–Ca–O, Cl–Ca–Cl, O–B–O and H–O–H angles 0.02, 0.01, 0.04, and 1.5° respectively. The conformation of the six-membered borate rings within the three pentaborate polyanions is given in Table 5.

### Absolute configuration

Since parahilgardite is triclinic noncentrosymmetric, two atomic configurations with respect to a right-handed coordinate system are possible, the first being represented by the  $x, y, z$  set and the second by the  $\bar{x}, \bar{y}, \bar{z}$  set of coordinates. To determine the absolute configuration, an independent least-squares refinement was carried out based on the  $\bar{x}, \bar{y}, \bar{z}$  set coordinates. After convergence, the resulting  $R$  factor (0.023) was considerably higher than that based on the  $x, y, z$  set of coordinates; hence, the latter set as listed in Table 1 represents the absolute configuration. It should be noted at this point that both left-handed and right-handed parahilgardite crystals occur in nature; so, the alternative configuration also exists.

### Description of the structure

#### The pentaborate framework

The crystal structure of parahilgardite consists of an open three-dimensional borate framework, where the calcium and chlorine atoms and water molecules occur within open channels. The building blocks of the framework are discrete  $[B_5O_{12}]^{9-}$  groups ( $5: 3T + 2\Delta$ )<sup>2</sup>. There are three such crystallographically distinct groups, which are designated here as polyanions in view of their hydrated analogs. Each of the three polyanions (A, B, C) with point symmetry  $I$  is formed by two six-membered boron-oxygen rings, joined through a common tetrahedral boron atom (Fig. 1). Each ring consists of two  $BO_4$  tetrahedra and a  $BO_3$  triangle. In the left-handed parahilgardite crystal used for the present structure determination, two of the polyanions (Fig. 1, a and c) exist in the left-handed ( $l$ ) and one (Fig 1b) in the right-handed ( $d$ ) configuration. In the corresponding right-handed crystal, the configurations are two  $d$  and one  $l$ .<sup>3</sup>

The two boron–oxygen rings within each polyanion deviate considerably from 90°; the angles between the two least-squares planes in polyanions A, B and C are 69.7, 53.4 and 84.9° (Table 5). Thus, the polyanion B appears to be the most distorted. This distortion also

Table 4. Parahilgardite:  $Ca_6[B_5O_9]_3Cl_3 \cdot 3H_2O$  interatomic distances and angles (with estimated standard deviations in parentheses)

Bond lengths (Å)		
B(1) - O(1) 1.388(4)	B(6) - O(10) 1.348(3)	B(11) - O(18) 1.351(3)
B(1) - O(2) 1.351(3)	B(6) - O(11) 1.382(3)	B(11) - O(20) 1.382(4)
B(1) - O(3) 1.370(4)	B(6) - O(12) 1.376(3)	B(11) - O(21) 1.374(4)
B(2) - O(3) 1.513(3)	B(7) - O(12) 1.518(3)	B(12) - O(21) 1.526(3)
B(2) - O(4) 1.507(2)	B(7) - O(13) 1.453(3)	B(12) - O(22) 1.488(2)
B(2) - O(5) 1.431(3)	B(7) - O(14) 1.437(3)	B(12) - O(23) 1.433(3)
B(2) - O(6) 1.458(3)	B(7) - O(15) 1.500(4)	B(12) - O(24) 1.459(3)
B(3) - O(1) 1.484(3)	B(8) - O(11) 1.484(3)	B(13) - O(20) 1.484(3)
B(3) - O(6) 1.434(4)	B(8) - O(13) 1.434(3)	B(13) - O(24) 1.437(4)
B(3) - O(7) 1.491(3)	B(8) - O(16) 1.471(4)	B(13) - O(25) 1.491(3)
B(3) - O(8) 1.473(3)	B(8) - O(17) 1.491(3)	B(13) - O(26) 1.469(3)
B(4) - O(5) 1.464(2)	B(9) - O(14) 1.472(3)	B(14) - O(2) 1.472(3)
B(4) - O(8) 1.465(4)	B(9) - O(16) 1.466(3)	B(14) - O(23) 1.467(2)
B(4) - O(9) 1.497(3)	B(9) - O(18) 1.467(3)	B(14) - O(26) 1.467(4)
B(4) - O(10) 1.467(3)	B(9) - O(19) 1.495(3)	B(14) - O(27) 1.494(3)
B(5) - O(4) 1.356(3)	B(10) - O(15) 1.350(2)	B(15) - O(22) 1.358(3)
B(5) - O(7) 1.362(4)	B(10) - O(17) 1.368(3)	B(15) - O(25) 1.364(4)
B(5) - O(9) 1.366(3)	B(10) - O(19) 1.365(3)	B(15) - O(27) 1.365(3)
Ca(1) - O(1) 2.502(2)	Ca(3) - O(6) 2.477(2)	Ca(5) - O(13) 2.486(2)
Ca(1) - O(2) 2.496(2)	Ca(3) - O(8) 2.515(2)	Ca(5) - O(16) 2.500(2)
Ca(1) - O(3) 2.435(2)	Ca(3) - O(10) 2.505(2)	Ca(5) - O(18) 2.513(2)
Ca(1) - O(5) 3.058(2)	Ca(3) - O(11) 2.506(2)	Ca(5) - O(20) 2.497(2)
Ca(1) - O(24) 2.467(2)	Ca(3) - O(12) 2.431(2)	Ca(5) - O(21) 2.435(2)
Ca(1) - O(26) 2.527(2)	Ca(3) - O(14) 3.070(2)	Ca(5) - O(23) 3.105(2)
Ca(1) - Cl(1) 2.775(1)	Ca(3) - Cl(2) 2.818(1)	Ca(5) - OW(3) 2.355(2)
Ca(1) - OW(1) 2.531(2)	Ca(3) - OW(2) 2.357(2)	Ca(5) - Cl(3) 2.822(1)
Ca(2) - O(1) 3.253(2)	Ca(4) - O(11) 3.183(2)	Ca(6) - O(20) 3.124(2)
Ca(2) - O(4) 2.587(2)	Ca(4) - O(13) 2.802(2)	Ca(6) - O(22) 2.556(2)
Ca(2) - O(5) 2.423(2)	Ca(4) - O(14) 2.411(2)	Ca(6) - O(23) 2.411(2)
Ca(2) - O(6) 2.798(2)	Ca(4) - O(15) 2.583(2)	Ca(6) - O(24) 2.803(2)
Ca(2) - O(7) 2.369(2)	Ca(4) - O(16) 2.591(2)	Ca(6) - O(25) 2.392(2)
Ca(2) - O(8) 2.573(2)	Ca(4) - O(17) 2.382(2)	Ca(6) - O(26) 2.620(2)
Ca(2) - O(9) 2.437(2)	Ca(4) - O(19) 2.433(2)	Ca(6) - O(27) 2.433(2)
Ca(2) - Cl(1) 2.763(1)	Ca(4) - Cl(2) 2.873(1)	Ca(6) - OW(1) 2.497(2)
Ca(2) - Cl(2) 2.909(1)	Ca(4) - Cl(3) 2.906(1)	Ca(6) - Cl(3) 2.867(1)
OW(1) - H(1) 1.01(6)	OW(2) - H(3) 1.00(7)	OW(3) - H(5) 0.97(6)
OW(1) - H(2) 1.01(7)	OW(2) - H(4) 0.96(5)	OW(3) - H(6) 1.03(7)
OW(1) - Cl(1) 3.345(3)	OW(2) - Cl(2) 3.283(3)	OW(3) - Cl(3) 3.265(3)
OW(1) - Cl(1) 3.207(3)	OW(2) - Cl(2) 3.173(3)	OW(3) - Cl(3) 3.185(3)
H(1) - Cl(1) 2.36(7)	H(3) - Cl(2) 2.32(7)	H(5) - Cl(3) 2.30(6)
H(2) - Cl(1) 2.24(6)	H(4) - Cl(2) 2.43(6)	H(6) - Cl(3) 2.29(6)
Ca(1) - OW(1) 2.531(2)	Ca(3) - OW(2) 2.357(2)	Ca(5) - OW(3) 2.355(2)
Ca(6) - OW(1) 2.497(2)		

#### Bond angles (°)

O(1) - B(1) - O(2) 112.8(2)	O(13) - B(7) - O(14) 112.2(2)
O(2) - B(1) - O(3) 125.7(3)	O(13) - B(7) - O(15) 106.0(2)
O(3) - B(1) - O(1) 121.1(2)	O(14) - B(7) - O(15) 115.4(1)
O(3) - B(2) - O(4) 105.0(1)	O(11) - B(8) - O(13) 112.8(2)

<sup>2</sup> Nomenclature after Christ and Clark (1977): 5: pentaborate, T: borate tetrahedron,  $\Delta$ : borate triangle.

<sup>3</sup> For a discussion of the stereoisomerism of the pentaborate polyanions and polymorphism of the hilgardite group of minerals, see Ghose (1982).

Table 4. (continued)

0(3) - B(2) - 0(5) 108.1(2)	0(11) - B(8) - 0(16) 109.3(2)
0(3) - B(2) - 0(6) 109.8(2)	0(11) - B(8) - 0(17) 108.9(2)
0(4) - B(2) - 0(5) 115.1(2)	0(13) - B(8) - 0(16) 110.1(2)
0(4) - B(2) - 0(6) 106.0(2)	0(13) - B(8) - 0(17) 104.8(2)
0(5) - B(2) - 0(6) 112.5(2)	0(16) - B(8) - 0(17) 110.8(2)
0(1) - B(3) - 0(6) 113.0(2)	0(14) - B(9) - 0(16) 107.1(2)
0(1) - B(3) - 0(7) 108.8(2)	0(14) - B(9) - 0(18) 108.8(2)
0(1) - B(3) - 0(8) 110.2(1)	0(14) - B(9) - 0(19) 110.7(2)
0(6) - B(3) - 0(7) 105.0(2)	0(16) - B(9) - 0(18) 110.8(2)
0(6) - B(3) - 0(8) 109.6(2)	0(16) - B(9) - 0(19) 111.6(2)
0(7) - B(3) - 0(5) 110.2(2)	0(15) - B(9) - 0(19) 107.9(2)
0(5) - B(4) - 0(8) 106.9(2)	0(15) - B(10) - 0(17) 124.1(3)
0(5) - B(4) - 0(9) 110.5(2)	0(17) - B(10) - 0(19) 120.6(2)
0(5) - B(4) - 0(10) 108.8(2)	0(19) - B(10) - 0(15) 115.3(2)
0(8) - B(4) - 0(9) 111.5(2)	0(18) - B(11) - 0(20) 112.7(2)
0(8) - B(4) - 0(10) 110.9(2)	0(20) - B(11) - 0(21) 120.9(2)
0(9) - B(4) - 0(10) 108.1(2)	0(21) - B(11) - 0(18) 126.2(3)
0(4) - B(5) - 0(7) 124.2(2)	0(21) - B(12) - 0(22) 105.7(1)
0(7) - B(5) - 0(9) 120.9(2)	0(21) - B(12) - 0(23) 108.1(2)
0(9) - B(5) - 0(4) 114.8(3)	0(21) - B(12) - 0(24) 108.9(2)
0(10) - B(6) - 0(11) 112.8(2)	0(22) - B(12) - 0(23) 115.0(2)
0(11) - B(6) - 0(12) 120.7(2)	0(22) - B(12) - 0(24) 106.4(2)
0(12) - B(6) - 0(10) 126.3(2)	0(23) - B(12) - 0(24) 112.4(2)
0(12) - B(7) - 0(13) 109.6(1)	0(20) - B(13) - 0(24) 112.7(2)
0(12) - B(7) - 0(14) 107.6(2)	0(20) - B(13) - 0(25) 109.3(2)
0(12) - B(7) - 0(15) 105.6(2)	0(20) - B(13) - 0(26) 109.7(1)
0(24) - B(13) - 0(25) 104.5(1)	0(23) - B(14) - 0(26) 107.5(2)
0(24) - B(13) - 0(26) 110.0(2)	0(23) - B(14) - 0(27) 110.0(2)
0(25) - B(13) - 0(26) 110.5(2)	0(26) - B(14) - 0(27) 111.4(2)
0(2) - B(14) - 0(23) 109.8(2)	0(22) - B(15) - 0(25) 124.4(2)
0(2) - B(14) - 0(26) 110.9(2)	0(25) - B(15) - 0(27) 121.2(2)
0(2) - B(14) - 0(27) 107.2(2)	0(27) - B(15) - 0(22) 114.4(3)
H(1) - OW(1) - H(2) 132(4)	OW(2) - H(3)...Cl(2) 161(4)
OW(1) - H(1)...Cl(1) 166(5)	OW(2) - H(4)...Cl(2) 135(5)
Ca(1) - OW(1) - H(2) 98(2)	Ca(3) - OW(2) - H(3) 111(3)
Ca(6) - OW(1) - H(1) 100(3)	Ca(3) - OW(2) - H(4) 118(4)
OW(1) - H(2)...Cl(1) 161(3)	H(5) - OW(3) - H(6) 133(4)
Ca(1) - OW(1) - H(1) 109(3)	OW(3) - H(5)...Cl(3) 173(4)
Ca(6) - OW(1) - H(2) 108(3)	OW(3) - H(6)...Cl(3) 145(3)
Ca(1) - OW(1) - Ca(6) 108.8(8)	Ca(5) - OW(3) - H(5) 113(3)
H(3) - OW(2) - H(4) 131(5)	Ca(5) - OW(3) - H(6) 112(3)

expresses itself in terms of the maximum deviation of the boron atoms from the mean ring planes, which are for polyanion A: +0.658 and +0.623Å; for polyanion B: +0.681 and +1.002Å; and for polyanion C: +0.698 and -0.619Å. The B-O-B angles within the rings vary from 112.9 to 123.5°. The average B-B separations with the two rings in polyanion A are: 2.455 and 2.471Å, in polyanion B: 2.447 and 2.473Å, and polyanion C: 2.449 and 2.467Å. In contrast, within the isolated pentaborate [B<sub>5</sub>O<sub>6</sub>(OH)<sub>6</sub>]<sup>3-</sup> polyanion in ulexite, the average B-B

Table 5. Ring angles, planes and deviations from ring planes for the borate polyanions in parahilgardite

Polyanion A			
Ring	Ring atoms	B-O-B angles(°)	
1	B(3)-0(1)-B(1)	B(3)-0(1)-B(1)	121.0(2)
	0(3)-B(2)-0(6)	B(1)-0(3)-B(2)	113.7(2)
2	B(3)-0(8)-B(4)	B(3)-0(8)-B(4)	114.9(2)
	0(9)-B(5)-0(7)	B(4)-0(9)-B(5)	123.5(2)
		B(5)-0(7)-B(3)	115.5(2)
Parameters of planes* defined by ring oxygens			
	A	B	C
1	5.2182	-4.7723	1.1058
2	16.5026	-0.9458	-0.8666
		D	0.9513
			2.2814
Angle between ring planes, 69.74°			
Deviations from ring planes defined by ring oxygens			
	Ring 1	Atom	Deviations (Å)
		B(3)	-0.054
		B(1)	-0.174
		B(2)	0.658
		O(2)	-0.388
		O(4)	2.048
		O(5)	0.599
	Ring 2	Atom	Deviations (Å)
		B(3)	0.048
		B(4)	0.623
		B(5)	-0.198
		O(4)	-0.669
		O(5)	-0.299
		O(10)	1.829
Polyanion B			
Ring	Ring atoms	B-O-B angles(°)	
3	B(8)-0(13)-B(7)-	B(8)-0(13)-B(7)	115.3(2)
	0(12)-B(6)-0(11)	B(7)-0(12)-B(6)	113.0(2)
4	B(8)-0(16)-B(9)-	B(8)-0(16)-B(9)	114.7(2)
	0(19)-B(10)-0(17)	B(9)-0(19)-B(10)	123.9(2)
		B(10)-0(17)-B(8)	115.7(2)
Parameters of planes* defined by ring oxygens			
	A	B	C
3	5.9297	5.8071	0.9385
4	15.0429	1.5043	-1.2634
		D	9.1000
			7.2221
Angle between ring planes, 53.38(°)			
Deviations from ring planes defined by ring oxygens			
	Ring 3	Atom	Deviations (Å)
		B(8)	-0.080
		B(7)	0.681
		B(6)	-0.212
		O(14)	0.656
		O(15)	2.046
		O(10)	-0.536
	Ring 4	Atom	Deviations (Å)
		B(8)	0.533
		B(9)	1.002
		B(10)	-0.383
		O(14) <sup>1</sup>	0.396
		O(18)	2.098
		O(15) <sup>1</sup>	-1.132
Polyanion C			
Ring	Ring atoms	B-O-B angles(°)	
5	B(13)-0(20)-B(11)-	B(13)-0(20)-B(11)	120.2(2)
	0(21)-B(12)-0(24)	B(11)-0(21)-B(12)	112.9(2)
6	B(13)-0(26)-B(14)-	B(13)-0(26)-B(14)	114.7(2)
	0(27)-B(15)-0(25)	B(14)-0(27)-B(15)	123.0(2)
		B(15)-0(25)-B(13)	115.4(2)
Parameters of planes* defined by ring oxygens			
	A	B	C
5	5.4658	-4.8840	0.8760
6	15.8343	2.1124	-0.2165
		D	4.4570
			14.0445
Angle between ring planes, 84.93°			

Continued on p. 608.

Table 5. (continued)

Deviations from ring planes defined by three oxygens			
Ring 5		Ring 6	
Atom	Deviation (Å)	Atom	Deviation (Å)
B(13)	-0.088	B(13)	-0.619
B(11)	-0.222	B(14)	-0.043
B(12)	0.698	B(15)	0.166
O(18)	-0.564	O(2)	1.111
O(22)	2.045	O(23)	-1.289
O(23)	0.704	O(22)	0.438

separations are 2.498 and 2.505 Å. Hence, the boron-oxygen rings in parahilgardite are considerably more distorted than those in ulexite, the distortion being comparable to that found in hilgardite (B-B separations 2.448 and 2.474 Å). The average tetrahedral and triangular B-O distances are 1.474 and 1.366 Å, which are in agreement with corresponding values found in numerous well-refined borate structures. However, within each borate tetrahedron there are two types of B-O bond lengths; those involving oxygens further bonded to a triangular boron (av. 1.492 Å) are in general larger than those involving oxygens further bonded to a tetrahedral boron (av. 1.455 Å). This difference is due to the fact that the triangular B-O bond has more covalent character than the tetrahedral B-O bond.

The three-dimensional framework can be considered to be constructed by further linkage of chains or layers formed by the linkage of the pentaborate polyanions. Chains parallel to the *c* axis are formed by sharing two tetrahedral borate corners with two other borate tetrahedra in adjacent polyanions. Three crystallographically

distinct chains, two left-handed and one right-handed, are formed this way (Fig. 2a,b,c). The backbone of each chain is a three-tetrahedral-repeat borate chain (*Dreier-einfachkette*), accounting for the 6.3 Å *c* axis. The configurations of the three different chains are very similar in terms of the B-B separations and B-B-B angles. The average values of three different B-B separations and B-B-B angles are 2.445, 2.501, 2.474 Å and 113.5, 138.9, 127.3°, respectively.

Within each borate chain, corners of two borate tetrahedra point along +*a* and +*b* directions, whereas corners of two borate triangles point along -*a* and -*b* directions; these corners are shared with four adjacent chains, such that tetrahedral corners of one chain are shared with triangular corners of the other (Fig. 3). The resulting open framework contains channels parallel to the *a*, *b* and *c* axes. The chlorine atoms and water molecules occur within straight channels parallel to the *c* axis, whereas the calcium atoms occur within zig-zag channels parallel to the *b* and *a* axes, respectively.

Alternatively, the framework structure can be considered as a stacking of the pentaborate layers formed by corner-sharing of the pentaborate chains along the *a* or *b* axes. Three stereochemically distinct pentaborate layers, two left-handed and one right-handed, each of which is formed by one of the three crystallographically distinct pentaborate polyanions, (Figs. 4a,b,c) are stacked along the *a* axis (Fig. 3). A comparable composite layer is formed by all three polyanion chains sharing corners along the *b* axis (Fig. 5). All four layers are characterized by large nine-membered rings, consisting of seven borate tetrahedra and two borate triangles.

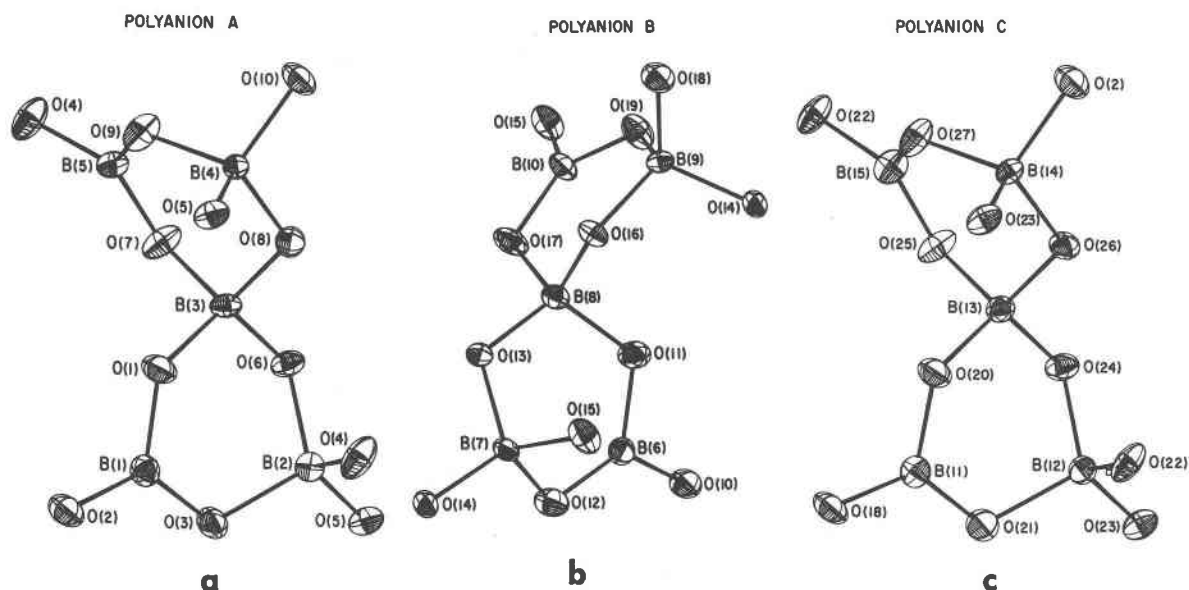


Fig. 1. Views of the three crystallographically distinct  $[B_5O_{12}]^{9-}$  polyanions in parahilgardite, showing the ellipsoids of thermal vibrations.

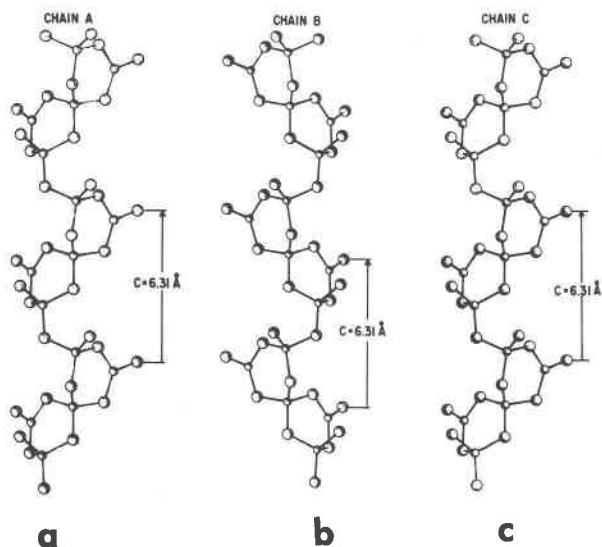


Fig. 2. The three crystallographically distinct three-tetrahedral-repeat pentaborate  $[B_5O_{11}]^{7-}$  chains in parahilgardite parallel to the  $c$  axis.

### The calcium polyhedral sheet

The calcium atoms occur within these large nine-membered borate rings, such that five or six nearly coplanar oxygen atoms are within  $3\text{\AA}$  of the Ca atom. The chlorine atom and the water molecule serve as apical

ligands. There are six independent Ca polyhedra (Fig. 6). The  $[Ca(1)O_6Cl(H_2O)]$ ,  $[Ca(2)O_6Cl_2]$ ,  $[Ca(3)O_6Cl(H_2O)]$ ,  $[Ca(5)O_6Cl(H_2O)]$  and  $[Ca(6)O_6Cl(H_2O)]$  polyhedra are all distorted hexagonal bipyramids. The exception to this rule is the  $[Ca(4)O_7Cl_2]$  polyhedron, which is a mono-capped hexagonal bipyramid. If we ignore the long  $Ca(4)-O(11)$  bond ( $3.18\text{\AA}$ ), it also becomes a hexagonal bipyramid. The average  $Ca-O$  distances within the six polyhedra Ca(1) through Ca(6) are:  $2.581$ ,  $2.431$ ,  $2.417$ ,  $2.626$ ,  $2.589$  and  $2.658\text{\AA}$ , respectively. The  $Ca-Cl$  (single or average of two) distances are  $2.775$ ,  $2.836$ ,  $2.818$ ,  $2.890$ ,  $2.822$  and  $2.867\text{\AA}$ . The apical  $Ca-OH_2$  distances within Ca(1), Ca(3), Ca(5) and Ca(6) polyhedra are  $2.531$ ,  $2.357$ ,  $2.355$  and  $2.497\text{\AA}$  respectively. The calcium polyhedra share corners, edges and faces to form linear chains parallel to  $[\bar{1}10]$ , which are connected by corner-sharing into elliptical twelve-membered rings and eventually into an open sheet (Fig. 7).

### Hydrogen bonding

Each water molecule is hydrogen-bonded to two adjacent chlorine atoms, forming quasi-linear chains parallel to the  $c$  axis (Fig. 8). There are three crystallographically independent hydrogen-bonded chains in parahilgardite, as opposed to a single one found in hilgardite. Because of the large thermal vibration of the water molecules, the accuracy of the determination of the hydrogen atom positions is not very high, and the  $H-O-H$  angles (av.  $132^\circ$ ) may be in considerable error. However, water molecules W(2) and W(3), which are bonded to one Ca

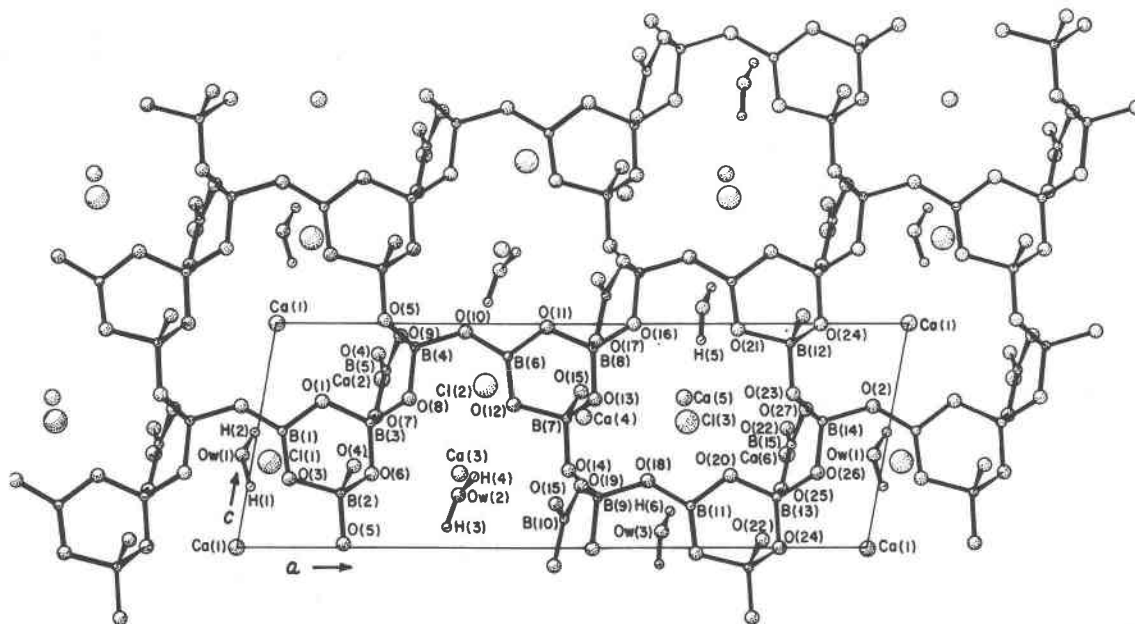


Fig. 3. A composite open pentaborate  $[B_5O_{11}]^{5-}$  layer in parahilgardite viewed down the  $b$  axis. This layer is formed by all three types of pentaborate polyanions. Note that the calcium atoms occur in open channels within the nine-membered rings formed by seven borate tetrahedra and two borate triangles.

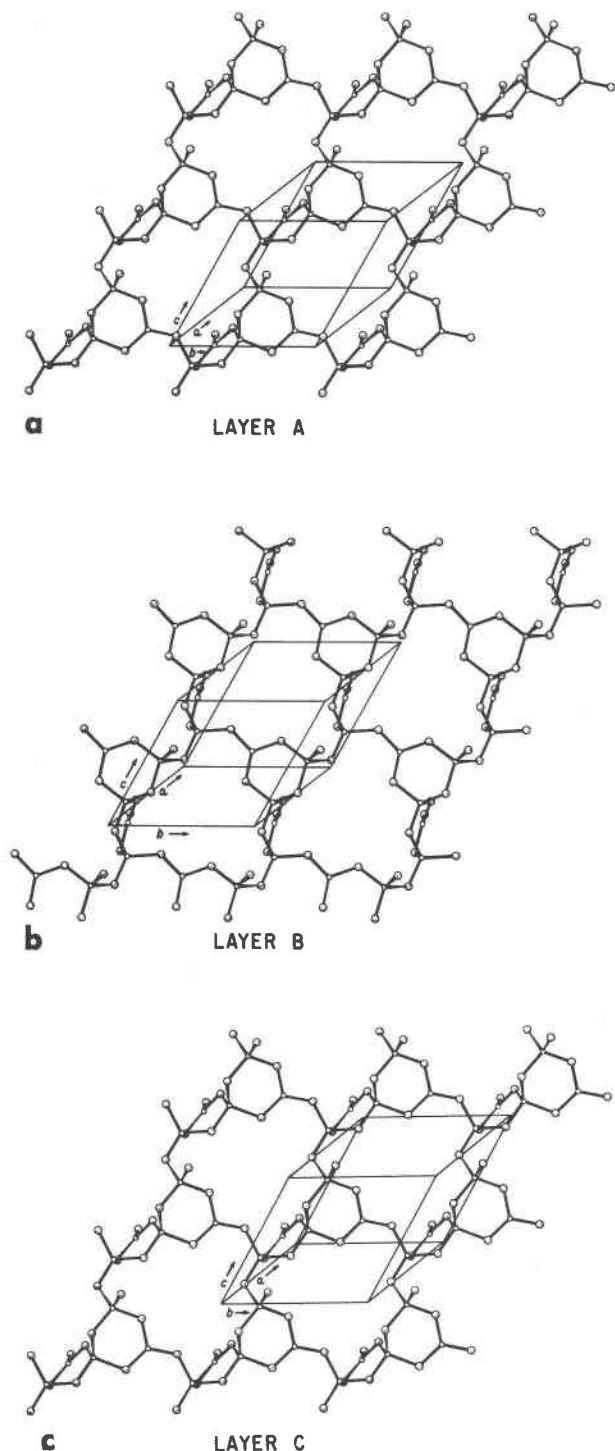


Fig. 4. The three crystallographically distinct open pentaborate  $[B_5O_{10}]^{5-}$  layers viewed down the  $a$  axis in parahilgardite. Each layer is formed by a crystallographically distinct polyanion. Note the nine-membered rings formed by seven borate tetrahedra and two borate triangles. The calcium atoms occur within the nine-membered rings (not shown).

atom each, are most likely in trigonal planar ( $sp^2$ ) configuration. On the other hand, the water molecule, W(1), which is bonded to two Ca atoms, in addition to being hydrogen-bonded to two chlorine atoms, is in the tetrahedral ( $sp^3$ ) configuration. Trigonal planar configurations of water molecules have also been found in hilgardite (Ghose and Wan, 1979) and hungchaoite,  $Mg(H_2O)_5 B_4O_5(OH_4) \cdot 2H_2O$ , a hydrogen bonded molecular complex (Wan and Ghose, 1977). In parahilgardite, the average O—H,  $H \cdots Cl$  and O(w)—Cl distances and O—H  $\cdots$  Cl angles are 1.00, 2.32, 3.243 Å and 157° respectively; the corresponding values in hilgardite are 0.93, 2.45, 3.229 Å and 146°.

The configuration of the chlorine atoms is of interest, since each of them is hydrogen bonded to two adjacent water molecules. Furthermore, Cl(2) and Cl(3) are bonded to three Ca atoms each, which lie in a plane, normal to the  $H \cdots Cl \cdots H$  direction, indicating a square-pyramidal coordination, where two hydrogen and two Ca atoms form the base and a Ca atom forms the apex. Cl(1) on the other hand is bonded to two Ca atoms instead of three and the configuration is a highly distorted tetrahedron.

#### Anisotropic thermal vibration

The thermal vibration of the tetrahedral boron atoms is nearly isotropic, whereas that of the triangular boron atoms is mildly anisotropic, the thermal vibration ellipsoid being a prolate spheroid with the direction of the largest vibration being normal to the borate triangle. The thermal vibrations of the oxygen atoms shared by two tetrahedral boron atoms are nearly isotropic or only mildly anisotropic; on the other hand the ellipsoids of the oxygen atoms shared between triangular and tetrahedral boron atoms are considerably more anisotropic, the largest vibration direction being normal to the B—O—B plane (Fig. 1). The ellipsoids for the calcium atoms are mildly anisotropic (Fig. 5). The largest anisotropic thermal vibrations are shown by the water molecules occurring in channels parallel to  $c$ , which are bonded to one or two calcium atoms each. The thermal vibration ellipsoids are large prolate spheroids, the largest vibration direction being normal to the Ca—O(w) direction or the Ca—O(w)—Ca plane. The anisotropic thermal vibration of the chlorine atoms, which are bonded to two or three calcium atoms each, are intermediate between those of the oxygen atoms and the water molecules.

#### Piezoelectricity in parahilgardite and its structural basis

G. W. Pierce (quoted in Hurlbut, 1938) positively determined the presence of piezoelectricity in parahilgardite, with a strong electric axis parallel or nearly parallel to the  $a$  axis. This phenomenon is very similar to that found in hilgardite. The origin of the piezoelectricity in parahilgardite lies in the way the borate tetrahedra and

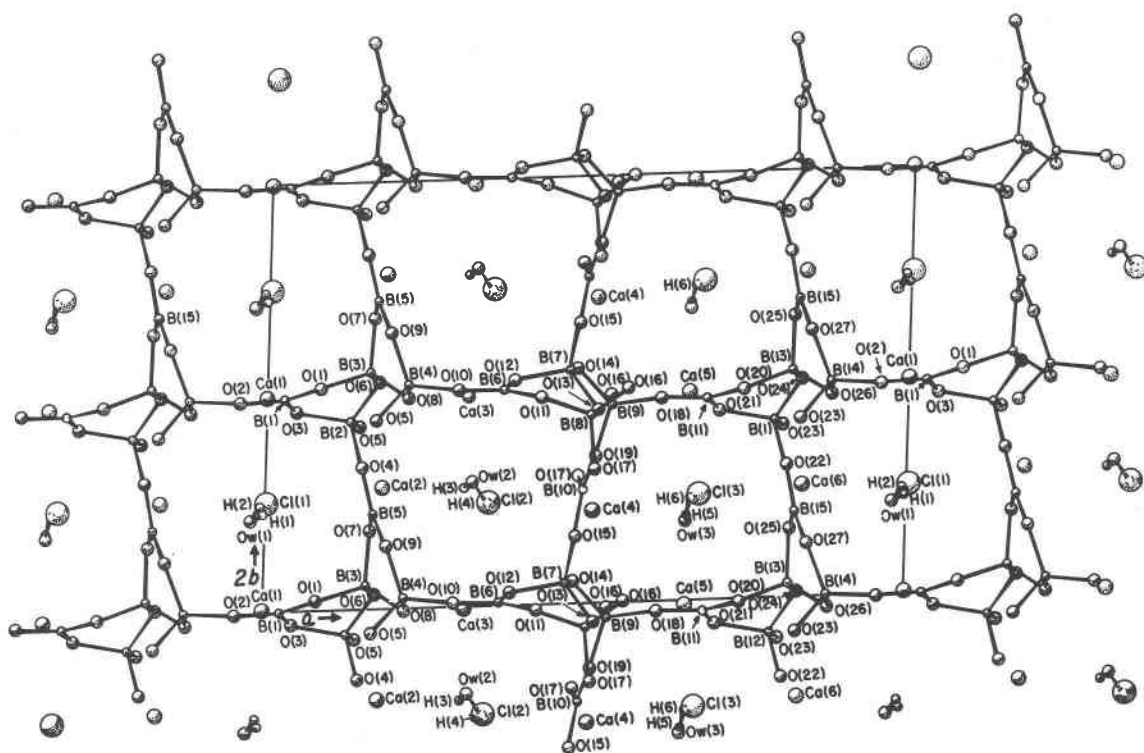


Fig. 5. The zeolite-type  $[B_5O_9]^{3-}$  framework in parahilgardite viewed down the  $c$  axis. Note the chlorine atoms and water molecules, which occur within open channels parallel to  $c$ .

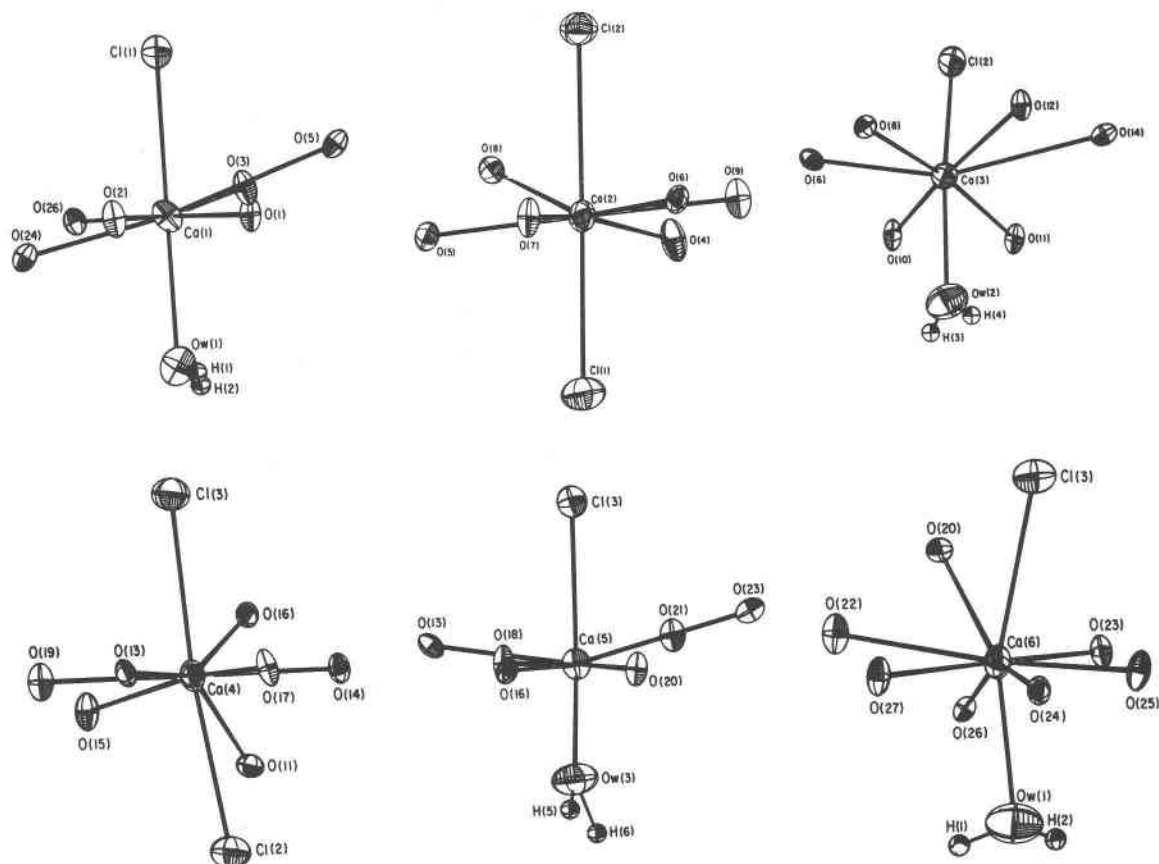


Fig. 6. The coordination polyhedra for the six crystallographically distinct calcium atoms, showing the ellipsoids of thermal vibration. Note the large anisotropic thermal vibration of the water molecules.

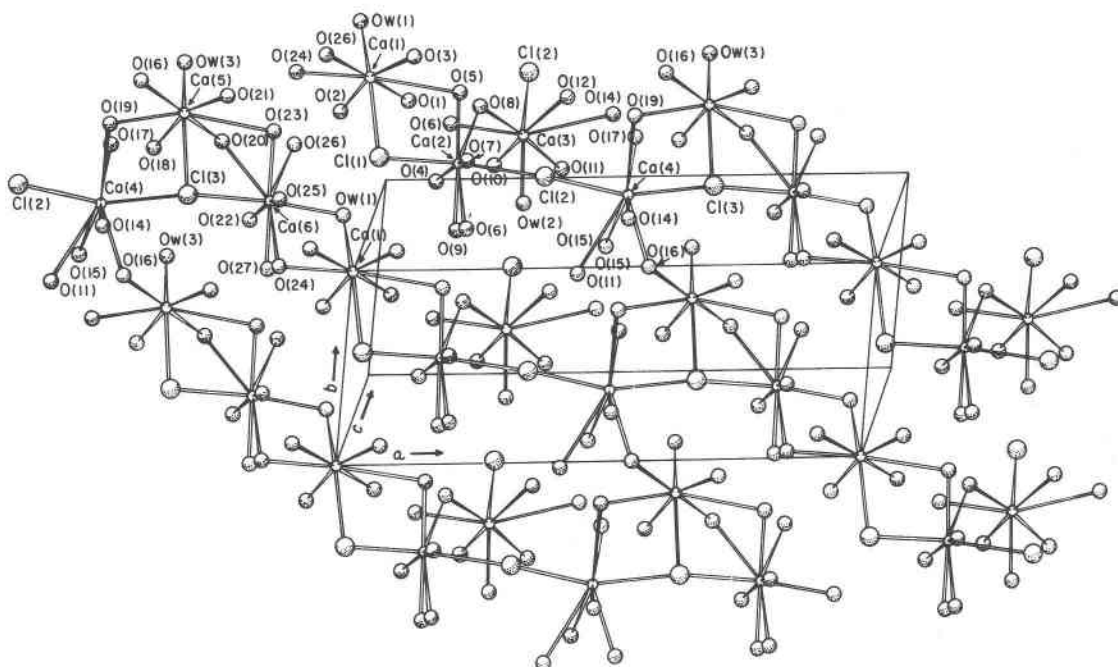


Fig. 7. The calcium polyhedral sheet in parahilgardite.

borate triangles are oriented within the structure (Fig. 3). Two borate triangles, B(5) and B(15) point along  $+b$ , whereas the borate triangle, B(10) points along  $-b$ . In contrast all the borate triangles, B(1), B(6) and B(11), point along  $-a$ . Hence, a maximum electric axis parallel to the  $a$  axis and an intermediate one parallel to the  $b$  axis

are expected. A minimum electric axis presumably exists parallel to the  $c$  axis, since all the borate tetrahedra point along  $-c$ .

#### Zeolite type pentaborate framework structures

The four known pentaborate framework structures found in  $\text{Ca}_2\text{B}_5\text{O}_9\text{Br}$  (Lloyd *et al.*, 1973), hilgardite,  $\text{Ca}_2\text{B}_5\text{O}_9\text{Cl} \cdot \text{H}_2\text{O}$  (Ghose and Wan, 1977, 1979), the triclinic hilgardite-type phase,  $\text{Ca}_2\text{B}_5\text{O}_9\text{Cl} \cdot \text{H}_2\text{O}$  (Rumanova *et al.*, 1977) and parahilgardite,  $\text{Ca}_6[\text{B}_5\text{O}_9]_3\text{Cl}_3 \cdot 3\text{H}_2\text{O}$  are all based on the same principle. In each case, the pentaborate polyanion chains parallel to the  $c$  axis ( $6.3\text{--}6.4\text{\AA}$ ) are connected to four adjacent chains by sharing tetrahedral borate corners with triangular ones along  $a$  and  $b$  axes, resulting in an open framework, characterized by straight (parallel to  $c$ ) and zig zag channels (parallel to  $a$  and  $b$ ), which house the calcium and halogen atoms and the water molecules. In all four structures the borate tetrahedra point along the  $+c$  or  $-c$  direction, whereas the orientation of the borate triangles along the  $a$  and  $b$  axes are quite different. The orientation of the borate triangles in parahilgardite has already been mentioned. In hilgardite, the borate triangles point along  $-a$ , and alternately along the  $+b$  and  $-b$  directions. In the triclinic hilgardite-type phase, they all point along the  $-a$  and  $-b$  (or  $+a$  and  $+b$ ) directions. In contrast, in  $\text{Ca}_2\text{B}_5\text{O}_9\text{Br}$ , they point alternately along  $+a$  and  $-a$ , and along  $+b$  and  $-b$ . As a result, in this compound no sizeable piezoelectric effect along the  $a$  and  $b$  axes is to be expected. Hence, the structure of  $\text{Ca}_2\text{B}_5\text{O}_9\text{Br}$  cannot be

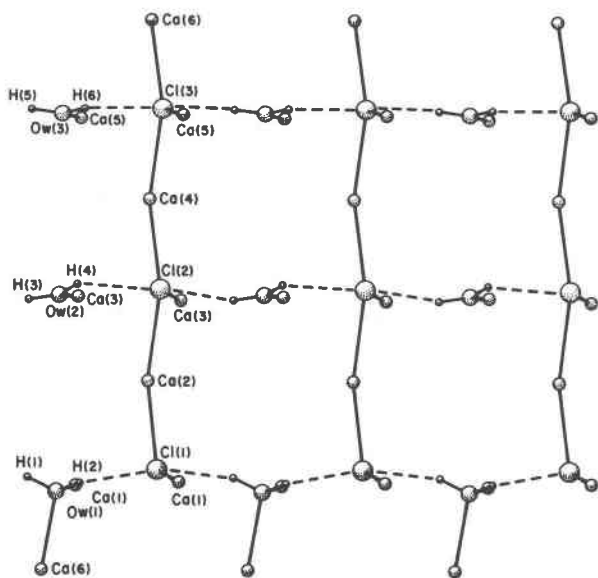


Fig. 8. The hydrogen bonded quasi-linear  $\text{Cl} \cdots \text{H}-\text{O} \cdots \text{H} \cdots \text{Cl}$  chains in parahilgardite, parallel to the  $c$  (horizontal) axis. Note the distorted tetrahedral coordination for Cl(1) and square-pyramidal coordination for Cl(2) and Cl(3).

considered simply as a dehydrated version of the hilgardite-type phase, as postulated by Lloyd *et al.*, (1973).

An interesting variation of the zeolite-type pentaborate structure is provided by  $K_2[B_5O_8(OH)] \cdot 2H_2O$  (Marezio, 1969). In this structure,  $[B_5O_8(OH)]^{2-}$  polyanions form sheets parallel to the (110) plane by sharing oxygens of borate triangles with those of borate tetrahedra; these sheets are hydrogen-bonded along the *a* direction to give rise to open channels parallel to the *b* axis, where the two water molecules are located.

### Acknowledgments

We are indebted to Dr. Joan R. Clark, formerly of the U.S. Geological Survey for the donation of the parahilgardite crystals, valuable discussions and a critical review, and to Floyd Bardsley, University of Washington for the diagrams. This research has been supported by the Graduate School Research Fund of the University of Washington and the NSF grants EAR 76-13373 and EAR 79-04886.

### References

- Burzlauff, H. (1967) Die Struktur des Heidornits  $Ca_3Na_2Cl(SO_4)_2B_5O_8(OH)_2$ . Neues Jahrbuch für Mineralogie, Monatshefte, 157–169.
- Braitsch, O. (1959) Tc-Strontiohilgardit  $(Ca,Sr)_2[B_5O_8(OH)_2Cl]$  und seine Stellung in der Hilgardit gruppe  $X_2^{II}[B_5O_8(OH)_2Cl]$ . Beiträge zur Mineralogie und Petrographie, 6, 233–247.
- Christ, C. L. (1960) Crystal chemistry and systematic classification of hydrated borate minerals. American Mineralogist, 45, 334–340.
- Christ, C. L. and Clark, J. R. (1977) A crystal-chemical classification of borate structures with emphasis on hydrated borates. Physics and Chemistry of Minerals, 2, 59–87.
- Clark, J. R. and Appleman, D. E. (1964) Pentaborate polyanion in the crystal structure of ulexite,  $NaCaB_5O_6(OH)_6 \cdot 5H_2O$ . Science, 145, 1295–1296.
- Cromer, D. T. and Liberman, D. (1970) Relativistic calculation of anomalous scattering factors for X-rays. Journal of Chemical Physics, 53, 1891–1898.
- Cromer, D. T. and Mann J. B. (1968) X-ray scattering factors computed from numerical Hartree-Fock wave functions. Acta Crystallographica, A24, 321–324.
- Ghose, S. (1982) Stereoisomerism of the pentaborate polyanion  $[B_5O_{12}]^{9-}$ , polymorphism and piezoelectricity in the hilgardite group of minerals: a novel class of polar borate zeolites. American Mineralogist, 67, 1265–1272.
- Ghose, S. and Wan, C. (1977) Hilgardite and parahilgardite piezoelectric zeolite type phases. Nature, 270, 594–595.
- Ghose, S. and Wan, C. (1979) Hilgardite,  $Ca_2[B_5O_9] \cdot H_2O$ : a piezoelectric zeolite-type pentaborate. American Mineralogist, 64, 187–195.
- Ghose, S., Wan, C., and Clark, J. R. (1978) Ulexite,  $NaCaB_5O_6(OH)_6 \cdot 5H_2O$ : structure refinement, polyanion configuration, hydrogen bonding and fiber optics. American Mineralogist, 63, 160–171.
- Hurlbut, Jr. C. S. (1938) Parahilgardite, a new triclinic pedial mineral. American Mineralogist, 23, 765–771.
- Hurlbut, Jr., C. S. and Taylor, R. E. (1937) Hilgardite, a new mineral species from Choctaw Salt Dome, Louisiana. American Mineralogist, 22, 1052–1957.
- Lloyd, D. J., Levasseur and Fouassier, C. (1973) Structure Cristalline du Bromoborate  $Ca_2B_5O_9Br$ . Journal of Solid State Chemistry, 6, 179–186.
- Marezio, M. (1969) The crystal structure of  $K_3[B_5O_8(OH)] \cdot 2H_2O$ . Acta Crystallographica, B25, 1787–1795.
- Menchetti, S. and Sabelli, C. (1977) The crystal structure of synthetic sodium pentaborate monohydrate. Acta Crystallographica, B33, 3730–3733.
- Rumanova, I. M., Kurbanov, Kh. M. and Belov, N. V. (1966) Crystal structure of probertite,  $CaNa[B_5O_7(OH)_4] \cdot 3H_2O$ . Soviet Physics Crystallography, 10, 513–522.
- Rumanova, I. M., Yorish, Z. I., and Belov, N. V. (1977) The crystal structure of triclinic hilgardite  $Ca_2[B_5O_9]Cl \cdot H_2O = Ca_2[B_3^I B_2^II O_9]Cl \cdot H_2O$ . Doklady Akademiia Nauk SSSR 236, 91–94 (in Russian).
- Stewart, R. F., Davidson, E. R., and Simpson, W. T. (1965) Coherent x-ray scattering for the hydrogen atom in the hydrogen molecule. Journal of Chemical Physics, 42, 3175–3187.
- Stewart, J. M., Kruger, G. J., Ammon, H. L., Dickinson, C., and Hall, S. R. (1972) The x-RAY SYSTEM—version of June 1972, Tech. Rep. TR-192, Computer Science Center, University of Maryland, College Park, MD.
- Wan, C. and Ghose, S. (1977) Hungchaoite,  $Mg(H_2O)_5 B_4O_5(OH)_4 \cdot 2H_2O$ : a hydrogen bonded molecular complex, American Mineralogist, 62, 1135–1143.

Manuscript received, November 9, 1982;  
accepted for publication, November 29, 1982.